Published in final edited form as:
Calcif Tissue Int. 2014 August ; 95(2): 125–131. doi:10.1007/s00223-014-9873-4.

Reduced tissue-level stiffness and mineralization in osteoporotic cancellous bone

Grace Kim[1], **Jacqueline H. Cole**[2], **Adele L. Boskey**[3,4,5], **Shefford P. Baker**[6], and **Marjolein C. H. van der Meulen**[1,3]

Grace Kim: gk242@cornell.edu; Jacqueline H. Cole: jacquecole@ncsu.edu; Adele L. Boskey: boskeya@hss.edu; Shefford P. Baker: shefford.baker@cornell.edu

[1]Sibley School of Mechanical and Aerospace Engineering, Cornell University, Ithaca, NY

[2]Department of Biomedical Engineering, University of North Carolina, Chapel Hill, NC

[3]Musculoskeletal Integrity Program, Hospital for Special Surgery, New York, NY

[4]Department of Biochemistry, Weill Medical College of Cornell University, New York, NY

[5]Graduate Program in Physiology, Biophysics, and Systems Biology, Weill Medical College of Cornell University, New York, NY

[6]Department of Materials Science and Engineering, Cornell University, Ithaca, NY

Abstract

Osteoporosis alters bone mass and composition ultimately increasing the fragility of primarily cancellous skeletal sites; however, effects of osteoporosis on tissue-level mechanical properties of cancellous bone are unknown. Dual-energy x-ray absorptiometry (DXA) scans are the clinical standard for diagnosing osteoporosis though changes in cancellous bone mass and mineralization are difficult to separate using this method. The goal of this study was to investigate possible difference in tissue-level properties with osteoporosis as defined by donor T-scores. Spine segments from Caucasian female cadavers (58–92 yrs) were used. A T-score for each donor was calculated from DXA scans to determine osteoporotic status. Tissue level composition and mechanical properties of vertebrae adjacent to the scan region were measured using nanoindentation and Raman spectroscopy. Based on T-scores, six samples were in the Osteoporotic group (58–74 yrs) and four samples were in the Not Osteoporotic group (65–92 yrs). The indentation modulus and mineral to matrix ratio (mineral:matrix) were lower in the Osteoporotic group than the Not Osteoporotic group. Mineral:matrix ratio decreased with age (r^2 = 0.35, p = 0.05), and the indentation modulus increased with a real bone mineral density (aBMD) (r^2 = 0.41, p = 0.04).

This study is the first to examine cancellous bone composition and mechanical properties from a fracture prone location with osteoporosis. We found differences in tissue composition and

Corresponding author: Marjolein C. H. van der Meulen, Sibley School of Mechanical and Aerospace Engineering, Cornell University, 219 Upson Hall, Ithaca, NY 14853, Tel: (607) 255-1445, Fax: (607) 255-1222, mcv3@cornell.edu.

Disclosures
None

mechanical properties with osteoporosis that could contribute to increased fragility in addition to changes in trabecular architecture and bone volume.

Keywords

Nanoindentation; Raman spectroscopy; Osteoporosis; Human trabecular bone

Introduction

The skeleton is a dynamic organ with temporal and spatial variations in composition, microarchitecture, and bone mass. In the healthy skeleton, variations in microarchitecture and tissue-level properties contribute to toughness and efficient load bearing ability [1]. Metabolic bone diseases such as osteoporosis can negatively alter bone composition and architecture. Changes due to osteoporosis are of particular interest because more than 2 million fragility fractures occur in men and women annually [2]. Osteoporosis was initially characterized as a disease of reduced bone mass. However, osteoporosis is now known not only to reduce bone mass, but also change trabecular architecture and alter bone tissue composition, ultimately making the bone more susceptible to fracture [3–5].

Areal bone mineral density (aBMD) as measured by dual-energy x-ray absorptiometry (DXA) is commonly used to assess fracture risk but has limited ability to predict fractures [6–7]. The disconnect between fracture risk and aBMD suggests that changes at the material level, in addition to the reduction in bone mass, could contribute to the increased fragility of primarily cancellous skeletal sites. A variety of compositional changes in cancellous bone have been previously associated with fragility-related fractures and osteoporosis. Cancellous bone biopsies from donors with previous fragility fractures had different ratios of non-reducible/reducible collagen cross-links compared with samples from donors without fractures [8] and decreased mineralization and carbonate substitution heterogeneity [5]. Reduced bone mineralization [9] and increased carbonate substitution and crystallinity have also been associated with osteoporosis [10–11]. The previously mentioned studies provided key information about compositional changes in bone tissue with osteoporosis, and tissue composition likely contributes to tissue-level mechanical properties; however, none of these studies examined tissue-level mechanical properties or confirmed the relationship between composition and material properties in osteoporotic tissue. In healthy and vitamin D deficient rodents, tissue composition has been related to changes in tissue-level mechanical properties [12–16]; however, a limited number of studies have looked at osteoporotic cancellous bone from humans [17–18], a relevant application of clinical interest.

The goal of this study was to examine the effects of osteoporosis on cancellous bone composition and mechanical properties at the tissue-level length scale and correlate changes in mechanical properties with changes in tissue composition at a site prone to fracture clinically. DXA scans of the L1–L4 vertebrae were performed on spine segments from female cadavers ranging from age 58 to 92 years to determine osteoporotic status based on T-scores. Due to the lack of age-matched samples the average age of the two groups were not equal. Compositional parameters (mineral:matrix ratio, crystallinity, and B-type

carbonate substitution) were measured using Raman microspectroscopy. Mechanical parameters (indentation modulus and hardness) were measured on the same cores using nanoindentation. Compositional and mechanical parameters were compared and correlated as a function of T-score.

Materials and Methods

Spine segments were obtained from 11 Caucasian female donors aged from 58 to 92 years. Ribs, additional vertebral levels that were outside T11-L4, and any portions of the pelvis were removed to allow the spine to rest in a flat position for the DXA scan. The spines were then refrozen. The frozen T11-L4 segments were secured in a curved Plexiglas® fixture, immersed in a saline bath within a Plexiglas® box, and scanned with a clinical fan-beam densitometer in lumbar spine array mode (Delphi QDR 4500A or QDR 4500W, Hologic Inc., Bedford, MA). aBMD was computed using standard manufacturer software for the L1–L4 region (n = 10). Based on the aBMD for each sample, the associated T-score was computed [19]. Using the definition of osteoporosis from the World Health Organization, the “Osteoporotic group” had 6 samples, all of which had T-scores of −2.5 or below. Four samples with T-scores greater than -2.5 were in the “Not Osteoporotic group”. Donor ages and T-scores for all samples are given in Table 1. The T-score, and osteoporotic status, for one sample could not be calculated due to a missing L1 vertebra. This sample was still used for tissue-level measurements and labeled as “N/A” in Figures 2 and 3. After scanning, a cylindrical core (diameter = 8.25 mm) was drilled from the centrum of each T12 vertebra (n = 11). The cores were dehydrated in a series of increasing ethanol concentrations and embedded in polymethylmethacrylate (PMMA). A 3-mm thick longitudinal section was removed from the central region of each core with a diamond saw and glued onto an atomic force microscope (AFM) stub. The samples were polished anhydrously on silicon carbide polishing paper lubricated with ethylene glycol and aluminum oxide-ethylene glycol slurries until the RMS surface roughness measured by AFM (Dimension 3100 Ambient AFM, Veeco, Plainview, NY) was less than 10 nm for a 5 μm by 5 μm region [20].

For each sample, three longitudinally oriented trabeculae were chosen for both nanoindentation and Raman microspectroscopy. To reduce intra-sample variability surface roughness was minimized by polishing the sample [20]. Care was taken to avoid trabeculae with scalloped surfaces indicative of active remodeling. A scanning nanoindenter (Triboindenter, Hysitron, Minneapolis, MN) with a Berkovich tip was used. Using the surface imaging capabilities of the indenter, lines of indentations were made perpendicular to the longitudinal axis of each trabecula, starting and ending 20 μm from the edges. Indentations were made at ~10 μm intervals while avoiding lacunae and pores visible on the surface. This sampling method resulted in at least 23 indentations per sample. Two loading protocols yielded different indentation depths, one for indentation analysis and one for visualization in Raman measurements. In 4 samples, small indents were created using a single trapezoidal load function with a maximum load of 500 μN, load/unload rates of ±50 μN/s, and a hold time of 10 s. The remaining 7 samples were loaded twice in succession with two trapezoidal load forms with peak loads of 500 followed by 1000 μN, both with load rates of ±50 μN//s and 10 s hold times. The larger 1000 μN indents were performed to make fiduciary markers on the sample for Raman spectroscopy. For all indents, indentation

modulus (E_i) and hardness (H) values were calculated from the unloading portion of the 500 μN indent using the Oliver-Pharr method [21]. Indentation modulus and hardness values were averaged, resulting in a single indentation modulus and hardness value for each sample.

Raman spectra from 800 cm^{-1} to 1800 cm^{-1} were collected using an optical microscope (inVia, Renishaw, Gloucestershire, UK) equipped with a 785-nm laser and a 50x, 0.75 N.A. objective. The resulting spot size was ~2 μm. The small indents were not visible with the microscope, so the laser was positioned at approximately the same location based on optical images of the samples. The large indents were visible with the microscope and used to position the laser such that the Raman spectra were collected from the exact same location as the indent. After the background fluorescence was subtracted (WiRE V2.0, Renishaw), the spectra were smoothed using a nine-point moving average, and peak heights were identified using in-house code (Matlab V7.0, The Mathworks, Inc.). Tissue mineralization was examined using the mineral-to-matrix ratio (mineral:matrix) calculated from the phosphate ν_1(~965 cm^{-1}) and CH_2 wag (~1450 cm^{-1}) peak heights, respectively [22–23]. Crystallinity was measured based on the full width at half maximum value of the phosphate ν_1 peak, with broader peaks representing lower crystallinity[24]. B-Type carbonate substitution was calculated from the peak height ratio of the carbonate peak (~1065 cm^{-1}) to phosphate ν_1 peak [22–23, 25].

Relationships between mechanical properties, composition, and age were assessed using simple and multiple linear regressions (JMP Pro 9, SAS, Cary, NC). Differences in compositional and mechanical parameters between the Osteoporotic and Not Osteoporotic groups were compared using the Wilcoxon Rank Sum test to account for non-normal distributions. Due to small samples sizes, statistical tables were used to determine the critical values for the Wilcoxon Rank Sum test. P-values less than or equal to 0.05 were considered significant.

Results

Samples were divided into two groups based on T-score, Osteoporotic and Not Osteoporotic, to compare differences in tissue-level properties with osteoporotic status (Figure 1). The average age of the osteoporotic group (79.7 ±11 yrs) was higher than the Not Osteoporotic group (66.5 ±8 yrs) ($p = 0.05$). The Osteoporotic group had a 14% lower indentation modulus ($p = 0.05$) and 21% lower mineral:matrix ratio ($p < 0.05$) than the Not Osteoporotic group. Hardness was not different between the two groups ($p > 0.05$).

Relationships between tissue-level composition and material properties were examined using simple and multiple linear regressions (Tables 2–3). The indentation modulus increased with rising mineral:matrix ratio ($r^2 = 0.47$, $p= 0.02$), but hardness did not (Figure 2, Table 2). Although crystallinity and carbonate substitution were not significant predictors of either nanoindentation outcome individually, crystallinity in addition to the mineral:matrix ratio concurrently explained 56% of the variability in indentation modulus (Adjusted $R^2 = 0.56$, $p = 0.06$) (Table 3). Carbonate substitution in addition to the mineral:matrix ratio explained 38% of the variability in hardness but was still not significant

(Adjusted R^2 = 0.38, p = 0.06) (Table 3). Combining all three compositional metrics did not improve the prediction of indentation modulus compared with crystallinity and mineral:matrix ratio.

Changes in age, aBMD, and tissue-level parameters were investigated using simple linear regressions. Tissue-level mineralization as measured by Raman spectroscopy tended to decrease with donor age (r^2 = 0.35, p = 0.05) (Figure 3). aBMD, Crystallinity, carbonate substitution, indentation modulus, and indentation hardness were not associated with age. Finally, relationships between tissue-level outcome measures and aBMD were investigated using simple linear regressions. The indentation modulus increased with rising aBMD (r^2 = 0.41, p=0.04) (Figure 4). No other tissue-level outcome measures varied with aBMD.

Discussion

The two goals of this study were to (1) investigate changes in tissue-level composition and mechanical properties with osteoporosis as defined by T-score and (2) determine the relationship between composition and tissue-level mechanical properties in human cancellous bone from a clinically relevant fracture site. Osteoporotic status was based on T-scores from DXA scans, and tissue-level analyses were performed on samples from adjacent vertebrae to those scanned using DXA. The T12 vertebra was chosen for material property analysis, as osteoporotic vertebral fractures often occur in the lower thoracic and upper lumbar spine regions [26–27]. The indentation modulus and mineral:matrix ratio of the Osteoporotic group were lower than the Not Osteoporotic group. With respect to relating compositional measures with mechanical properties, the mineral:matrix ratio best predicted both the indentation modulus and hardness, and the addition of other compositional measures, crystallinity and B-type carbonate substitution, improved the prediction for the indentation modulus and hardness, respectively.

Animal studies of postmenopausal bone loss had mixed results regarding changes in material properties as assessed by nanoindentation. One study found no difference in indentation modulus or hardness of vertebral cancellous bone 20 weeks after ovariectomy [28], and another found a decrease in indentation modulus and hardness 16 weeks after ovariectomy [29], but these discrepancies could be due to differences in hydration of the test samples.

Previous studies of human cancellous bone from the iliac crest found nanoindentation outcome measures to be insensitive to fragility fracture [17] and menopause [18]. Composition of cancellous bone varies across skeletal sites in healthy bone [30–31], and osteoporosis affects different skeletal sites at different rates [32]. Thus comparing changes in tissue-level properties of cancellous bone from the iliac crest with cancellous bone from the spine may not be suitable. A study examining human cortical bone from the femoral neck found no differences in nanoindentation outcome measures between donors that suffered a fragility fracture and age matched controls despite reduced mineralization values [33]. This finding is unexpected because numerous studies have reported positive linear correlations between mineralization and nanoindentation measures [12–16, 34]. Alternatively, the lack of

difference in nanoindentation outcomes found by Fratzl-Zelman suggests other mechanical properties such as fracture toughness or strength may better explain bone fragility.

Microindentation has also been used to measure the hardness of iliac crest bone from osteoporotic men and women [34]. This study found lower Vicker's microhardness and degree of mineralization of bone (DMB) in samples from osteoporotic men than from control men, but there were no differences between samples from control and osteoporotic women. The coefficient of determination between mechanical properties (Vicker's Hardness) and mineralization (DMB) for men ($r^2 = 0.52$) and women ($r^2 = 0.4$) were similar to the current study [34]. Previous studies and the current study have reported reduced mineralization of samples from women with osteoporosis and fragility fractures [9, 33]. It is not clear why the microhardness study did not have differences in mineralization with osteoporosis in the samples from women.

Correlations between aBMD and tissue-level properties in the current study are particularly interesting because aBMD is a clinically used criterion for diagnosing osteoporosis. Despite the widespread clinical use and acceptance of DXA, aBMD does not always predict fracture [35–36] and the use of urinary bone turnover markers and various risk factors in addition to aBMD can improve fracture risk assessment in post-menopausal women [37–38]. To extrapolate the relationships between material properties and aBMD found in this study to implications for fracture risk, patient fracture history or bone turnover markers would be a valuable supplement to aBMD data. However, such clinical information was not available for the cadaver bone used in this study.

In addition to differences in indentation modulus and mineralization, the average age also differed between the Osteoporotic and Not Osteoporotic groups. Though the use of age-matched samples was not possible in this study, the linear regression analysis provides some insight regarding the contribution of aging and osteoporosis to differences in mineralization and indentation modulus between the two groups. In the current study a negative linear relationship between mineralization and age was found (Figure 3), making it difficult to distinguish if reduced mineralization was related to age or T-score. However for the indentation modulus and T-score there was no correlation with age suggesting the difference in indentation modulus between groups was likely not due to age.

An additional compositional parameter that may explain the changes in mechanical properties is collagen cross-linking. Collagen cross-linking ratios change with osteoporosis and are correlated to the mechanical behavior of bone tissue [8, 39–40]. Collagen cross-links were not characterized in this study due to overlapping peaks from the embedding medium and known changes in the Amide I and III regions with plastic deformation [41]. However, the use of FTIR spectroscopy before indentation would allow for collagen cross-link evaluation in the future.

This study is the first to examine osteoporotic cancellous bone composition and mechanical properties from a site prone to osteoporotic fracture. The indentation modulus was reduced in osteoporotic human cancellous bone from a lower thoracic vertebra. The reduced indentation modulus coincided with decreased mineralization and increased crystallinity and

carbonate substitution. Whole bone strength depends on bone mass, architecture and material properties. Bone volume fraction, as measured by micro-computed tomography scans, predicts 73–97% of the ultimate stress and Young's Modulus of vertebral cancellous bone [42–44]. Though cancellous architecture and bone mass are clearly important to whole bone strength, the contribution of material properties should not be overlooked. Because material properties are independent of bone mass and architecture metrics, the differences in material properties between osteoporotic and non-osteoporotic bone tissue could contribute to the remaining 3–27% of the variability in apparent level strength and stiffness. Future work examining cancellous architecture and apparent-level mechanical properties concurrently with tissue-level properties will provide a complete quantitative assessment of the influence of material properties on apparent level mechanical properties. Future therapies designed not only to increase bone mass but also optimize tissue material properties could offer even more effective therapies for osteoporosis and fracture risk prevention.

Acknowledgments

This study was supported by NIH/NAIMS grant P30-AR046121, R01-AR053571, R01-AR041325 and T32-AR007281. This work made use of the Cornell Center for Materials Research Facilities supported by the National Science Foundation under Award Number DMR-0520404. The authors would like to thank HysitronInc for use of the nanoindenter.

References

1. Tai K, Dao M, Suresh S, Palazoglu A, Ortiz C. Nanoscale heterogeneity promotes energy dissipation in bone. Nat Mater. 2007; 6:454–462. [PubMed: 17515917]
2. Burge R, Dawson-Hughes B, Solomon DH, Wong JB, King A, Tosteson A. Incidence and Economic Burden of Osteoporosis-Related Fractures in the United States, 2005–2025. J Bone Miner Res. 2007; 22:465–475. [PubMed: 17144789]
3. Boutroy S, Bouxsein ML, Munoz F, Delmas PD. In vivo assessment of trabecular bone microarchitecture by high-resolution peripheral quantitative computed tomography. J Clin Endocrinol Metab. 2005; 90:6508–6515. [PubMed: 16189253]
4. Legrand E, Chappard D, Pascaretti C, Duquenne M, Krebs S, Rohmer V, Basle M-F, Audran M. Trabecular Bone Microarchitecture, Bone Mineral Density, and Vertebral Fractures in Male Osteoporosis. J Bone Miner Res. 2000; 15:13–19. [PubMed: 10646109]
5. Gourion-Arsiquaud S, Lukashova L, Power J, Loveridge N, Reeve J, Boskey AL. Fourier transformed infra-red imaging of femoral neck bone: Reduced heterogeneity of mineral-to-matrix and carbonate-to-phosphate and more variable crystallinity in treatment-naïve fracture cases compared to fracture-free controls. J Bone Miner Res. 2012:n/a–n/a.
6. Miller PD, Siris ES, Barrett-Connor E, Faulkner KG, Wehren LE, Abbott TA, Chen YT, Berger ML, Santora AC, Sherwood LM. Prediction of fracture risk in postmenopausal white women with peripheral bone densitometry: evidence from the National Osteoporosis Risk Assessment. J Bone Miner Res. 2002; 17:2222–2230. [PubMed: 12469916]
7. Marshall D, Johnell O, Wedel H. Meta-analysis of how well measures of bone mineral density predict occurrence of osteoporotic fractures. BMJ. 1996; 312:1254–1259. [PubMed: 8634613]
8. Gourion-Arsiquaud S, Faibish D, Myers E, Spevak L, Compston J, Hodsman A, Shane E, Recker RR, Boskey ER, Boskey AL. Use of FTIR Spectroscopic Imaging to Identify Parameters Associated With Fragility Fracture. J Bone Miner Res. 2009; 24:1565–1571. [PubMed: 19419303]
9. Boivin GY, Chavassieux PM, Santora AC, Yates J, Meunier PJ. Alendronate increases bone strength by increasing the mean degree of mineralization of bone tissue in osteoporotic women. Bone. 2000; 27:687–694. [PubMed: 11062357]

10. Boskey AL, DiCarlo E, Paschalis E, West P, Mendelsohn R. Comparison of mineral quality and quantity in iliac crest biopsies from high-and low-turnover osteoporosis: an FT-IR microspectroscopic investigation. Osteoporos Int. 2005; 16:2031–2038. [PubMed: 16088360]
11. McCreadie BR, Morris MD, Chen T-c, Sudhaker Rao D, Finney WF, Widjaja E, Goldstein SA. Bone tissue compositional differences in women with and without osteoporotic fracture. Bone. 2006; 39:1190–1195. [PubMed: 16901772]
12. Busa B, Miller LM, Rubin CT, Qin YX, Judex S. Rapid establishment of chemical and mechanical properties during lamellar bone formation. Calcif Tissue Int. 2005; 77:386–394. [PubMed: 16362460]
13. Miller LM, Little W, Schirmer A, Sheik F, Busa B, Judex S. Accretion of bone quantity and quality in the developing mouse skeleton. J Bone Miner Res. 2007; 22:1037–1045. [PubMed: 17402847]
14. Donnelly E, Chen D, Boskey AL, Baker SP, van der Meulen MCH. Contribution of Mineral to Bone Structural Behavior and Tissue Mechanical Properties. Calcif Tissue Int. 2010; 87:450–460. [PubMed: 20730582]
15. Burket J, Gourion-Arsiquaud S, Havill LM, Baker SP, Boskey AL, van der Meulen MCH. Microstructure and nanomechanical properties in osteons relate to tissue and animal age. J Biomech. 2011; 44:277–284. [PubMed: 21074774]
16. Kim G, Boskey AL, Baker SP, van der Meulen MCH. Improved prediction of rat cortical bone mechanical behavior using composite beam theory to integrate tissue level properties. J Biomech. 2012; 45:2784–2790. [PubMed: 23021607]
17. Wang X, Sudhaker Rao D, Ajdelsztajn L, Ciarelli TE, Lavernia EJ, Fyhrie DP. Human iliac crest cancellous bone elastic modulus and hardness differ with bone formation rate per bone surface but not by existence of prevalent vertebral fracture. Journal of Biomedical Materials Research Part B: Applied Biomaterials. 2008; 85B:68–77.
18. Polly B, Yuya P, Akhter M, Recker R, Turner J. Intrinsic Material Properties of Trabecular Bone by Nanoindentation Testing of Biopsies Taken from Healthy Women Before and After Menopause. Calcif Tissue Int. 2012; 90:286–293. [PubMed: 22349078]
19. Kanis JA, Melton LJ, Christiansen C, Johnston CC, Khaltaev N. The diagnosis of osteoporosis. J Bone Miner Res. 1994; 9:1137–1141. [PubMed: 7976495]
20. Donnelly E, Baker SP, Boskey AL, van der Meulen MCH. Effects of surface roughness and maximum load on the mechanical properties of cancellous bone measured by nanoindentation. Journal of Biomedical Materials Research Part A. 2006; 77:426–435. [PubMed: 16392128]
21. Oliver WC, Pharr GM. Improved technique for determining hardness and elastic modulus using load and displacement sensing indentation experiments. Journal of Materials Research. 1992; 7:1564–1583.
22. Carden A, Morris MD. Application of vibrational spectroscopy to the study of mineralized tissues (review). J Biomed Opt. 2000; 5:259. [PubMed: 10958610]
23. Timlin JA, Carden A, Morris MD, Bonadio JF, Hoffler CE II, Kozloff KM, Goldstein SA. Spatial distribution of phosphate species in mature and newly generated mammalian bone by hyperspectral Raman imaging. J Biomed Opt. 1999; 4:28. [PubMed: 23015166]
24. Freeman JJ, Wopenka B, Silva MJ, Pasteris JD. Raman spectroscopic detection of changes in bioapatite in mouse femora as a function of age and in vitro fluoride treatment. Calcif Tissue Int. 2001; 68:156–162. [PubMed: 11351499]
25. Turunen MJ, Saarakkala S, Rieppo L, Helminen HJ, Jurvelin JS, Isaksson H. Comparison between infrared and Raman spectroscopic analysis of maturing rabbit cortical bone. Applied Spectroscopy. 2011; 65:595–603. [PubMed: 21639980]
26. Johansson C, Mellstrom D, Rosengren K, Rundgren Å. A Community-based Population Study of Vertebral Fractures in 85-year-old Men and Women. Age Ageing. 1994; 23:388–392. [PubMed: 7825484]
27. Black DM, Cummings SR, Stone K, Hudes E, Palermo L, Steiger P. A new approach to defining normal vertebral dimensions. J Bone Miner Res. 1991; 6:883–892. [PubMed: 1785377]
28. Guo XE, Goldstein SA. Vertebral trabecular bone microscopic tissue elastic modulus and hardness do not change in ovariectomized rats. J Orthop Res. 2000; 18:333–336. [PubMed: 10815837]

29. Maïmoun L, Brennan-Speranza TC, Rizzoli R, Ammann P. Effects of ovariectomy on the changes in microarchitecture and material level properties in response to hind leg disuse in female rats. Bone. 2012; 51:586–591. [PubMed: 22580391]
30. Donnelly E, Meredith DS, Nguyen JT, Boskey AL. Bone tissue composition varies across anatomic sites in the proximal femur and the iliac crest. J Orthop Res. 2012
31. Aerssens J, Boonen S, Joly J, Dequeker J. Variations in trabecular bone composition with anatomical site and age: potential implications for bone quality assessment. J Endocrinol. 1997; 155:411–421. [PubMed: 9487986]
32. Davis JW, Ross PD, Wasnich RD. Evidence for both generalized and regional low bone mass among elderly women. J Bone Miner Res. 1994; 9:305–309. [PubMed: 8191922]
33. Fratzl-Zelman N, Roschger P, Gourrier A, Weber M, Misof BM, Loveridge N, Reeve J, Klaushofer K, Fratzl P. Combination of nanoindentation and quantitative backscattered electron imaging revealed altered bone material properties associated with femoral neck fragility. Calcif Tissue Int. 2009; 85:335–343. [PubMed: 19756347]
34. Boivin G, Bala Y, Doublier A, Farlay D, Ste-Marie L, Meunier P, Delmas P. The role of mineralization and organic matrix in the microhardness of bone tissue from controls and osteoporotic patients. Bone. 2008; 43:532–538. [PubMed: 18599391]
35. Cummings SR, Karpf DB, Harris F, Genant HK, Ensrud K, LaCroix AZ, Black DM. Improvement in spine bone density and reduction in risk of vertebral fractures during treatment with antiresorptive drugs. The American journal of medicine. 2002; 112:281–289. [PubMed: 11893367]
36. Riggs B, Wahner H, Dunn W, Mazess R, Offord K, Melton L. Differential changes in bone mineral density of the appendicular and axial skeleton with aging: relationship to spinal osteoporosis. J Clin Invest. 1981; 67:328. [PubMed: 7462421]
37. Garnero P, Hausherr E, Chapuy MC, Marcelli C, Grandjean H, Muller C, Cormier C, Bréart G, Meunier PJ, Delmas PD. Markers of bone resorption predict hip fracture in elderly women: The EPIDOS prospective study. J Bone Miner Res. 1996; 11:1531–1538. [PubMed: 8889854]
38. Kanis J, Johnell O, Odén A, Johansson H, McCloskey E. FRAX™ and the assessment of fracture probability in men and women from the UK. Osteoporos Int. 2008; 19:385–397. [PubMed: 18292978]
39. Vashishth D, Gibson G, Khoury J, Schaffler M, Kimura J, Fyhrie D. Influence of nonenzymatic glycation on biomechanical properties of cortical bone. Bone. 2001; 28:195–201. [PubMed: 11182378]
40. Saito M, Marumo K. Collagen cross-links as a determinant of bone quality: a possible explanation for bone fragility in aging, osteoporosis, and diabetes mellitus. Osteoporos Int. 2010; 21:195–214. [PubMed: 19760059]
41. Carden A, Rajachar RM, Morris MD, Kohn DH. Ultrastructural changes accompanying the mechanical deformation of bone tissue: a Raman imaging study. Calcif Tissue Int. 2003; 72:166–175. [PubMed: 12469250]
42. Nazarian A, von Stechow D, Zurakowski D, Müller R, Snyder BD. Bone volume fraction explains the variation in strength and stiffness of cancellous bone affected by metastatic cancer and osteoporosis. Calcif Tissue Int. 2008; 83:368–379. [PubMed: 18946628]
43. Homminga J, Mccreadie BR, Weinans H, Huiskes R. The dependence of the elastic properties of osteoporotic cancellous bone on volume fraction and fabric. J Biomech. 2003; 36:1461–1467. [PubMed: 14499295]
44. Morgan EF, Bayraktar HH, Keaveny TM. Trabecular bone modulus–density relationships depend on anatomic site. J Biomech. 2003; 36:897–904. [PubMed: 12757797]

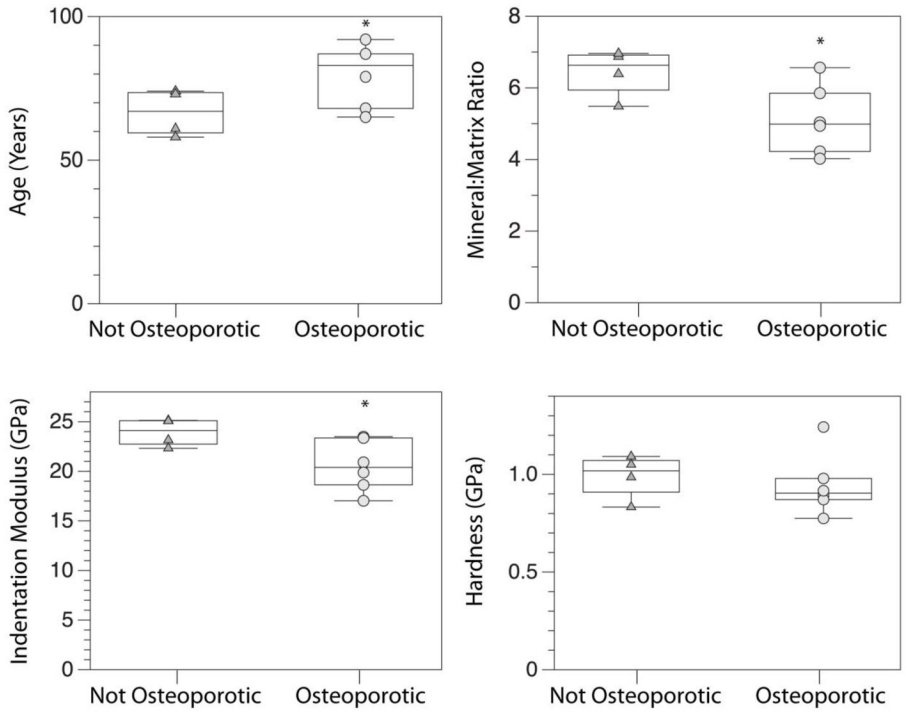

Figure 1.

Box-and-whisker plots for a) Age, b) mineral:matrix ratio, c) indentation modulus, and d) hardness for the Not Osteoporotic and Osteoporotic groups.*indicates different from Not Osteoporotic, $p \leq 0.05$.

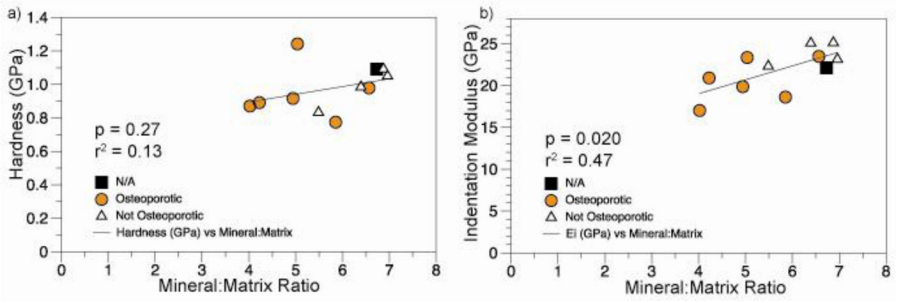

Figure 2.

Linear regressions of a) indentation modulus and b) hardness with tissue mineralization. Changes in hardness were not associated with changes in the mineral:matrix ratio, but the indentation modulus increased with increasing mineralization.

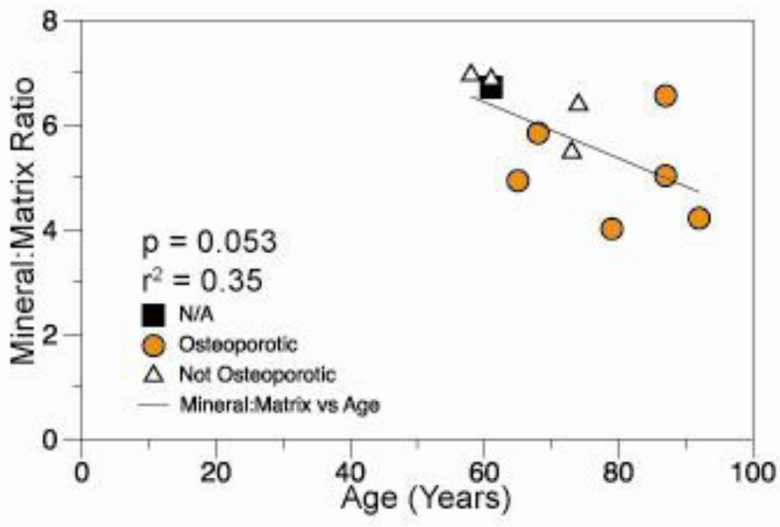

Figure 3.

Linear regression of tissue-level mineralization as measured by Raman spectroscopy with age.

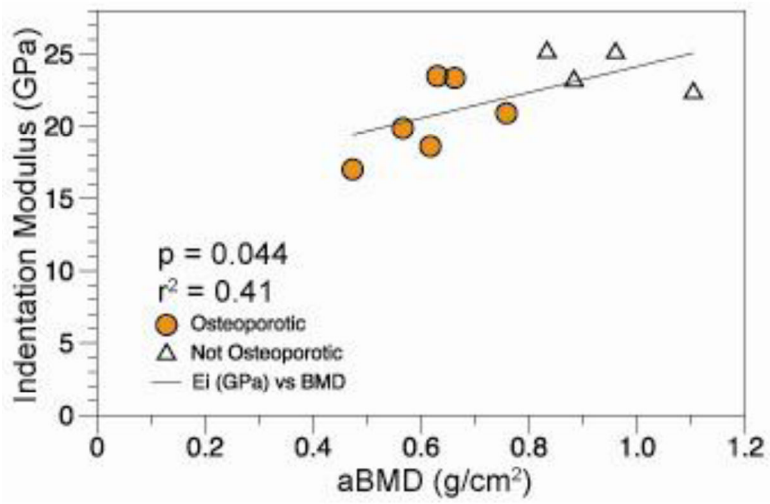

Figure 4.
Linear regression of the indentation modulus with mineralization as measured by DXA.

Table 1

Age and T-score for all samples.

Sample	Age (Years)	L1–L4 T-score
4	61	Not Available
7	87	−3.8
9	87	−3.5
11	61	−1.9
15	92	−2.6
20	74	−0.8
24	58	−1.5
30	73	0.5
31	79	−5.2
36	68	−3.9
37	65	−4.4

Table 2

Correlation coefficients, coefficients of determination, and p-values for simple linear regression of tissue-level properties and aBMD.

Predictor	Response	r	r^2	p
Mineral:Matrix	Age	−0.60	0.35	0.053
E_i (GPa)	aBMD L1–L4	0.64	0.41	0.044
E_i (GPa)	Mineral:Matrix	0.69	0.47	0.020
H (GPa)	Mineral:Matrix	0.36	0.13	0.27
H (GPa)	Ei	0.63	0.40	0.036

Table 3

Adjusted coefficients of determination and associated p-values for multiple linear regressions to predict tissue-level mechanical properties (Indentation modulus (E_i) and Hardness (H)).

Dependent Variable	Independent Variable	R^2	p
	Mineral:Matrix, Crystallinity	0.56	0.015
H	Mineral:Matrix, Carbonate Substitution	0.38	0.062